Characterizing Disjoining Pressure of Water in SiO_2 Nanochannels by Wicking Experiments

CNF Project Number: 2123-12

Principal Investigator(s): Shalabh C. Maroo

User(s): An Zou, Durgesh Ranjan

Affiliation(s): Department of Mechanical and Aerospace Engineering, Syracuse University, Syracuse, NY 13244

Primary Source(s) of Research Funding: National Science Foundation Career Award NO. 1454450; Office of Naval Research Grant NO. N000141812357

Contact(s): scmaroo@syr.edu, azou@syr.edu, dranjan@syr.edu

Website: http://maroo.syr.edu

Primary CNF Tools Used: Heidelberg mask writer - DWL2000, manual photoresist spinner, Gamma coat-develop tool, GCA auto stepper, ASML stepper, YES image reversal oven, ABM contact aligner, SÜSS MA6-BA6 contact aligner, e-beam evaporator, Oxford PECVD, GSI PECVD, Glen 1000 Plasma, Anatech resist strip, Oxford 81/82/100 etchers, P-T deep silicon etcher, Unaxis 770 deep silicon etcher, optical microscope, SEM, AFM

Abstract:

We characterized disjoining pressure of water in SiO_2 nanochannels by studying water wicking in 59 nm channels. The wicking in nanochannels was dominated by disjoining pressure. Wicking distance is proportional to square root of time, and the slope can be used to calculate the disjoining pressure, which can be as high as ~ 1.5 MPa in 59 nm channel. The work reported here is part of an article that is currently under review [1].

Summary of Research:

The pressure in a thin liquid film, with thicknesses ranged from a few nanometers to hundreds of nanometers, differs from its bulk due to the considerable, if not dominant, intermolecular interactions. This pressure difference is characterized by disjoining pressure, which plays a fundamental role in a wide range of engineering and natural systems involving bubbles, foams, emulsions, and membrane, etc. Since disjoining pressure is originated from intermolecular interactions, it is significantly affected by the material of surrounding surfaces, which could be any combination of solid, liquid, and vapor. Although disjoining pressure in a non-polar liquid film has been well understood, comprehensive knowledge for polar liquids, like water on a silicon dioxide (SiO_2) surface, is still lacking. Here, we report an experimental characterization of disjoining pressure of water in 1D SiO_2 nanochannels (height: 59 nm) with all walls made of SiO_2, by studying the water wicking process in nanochannels.

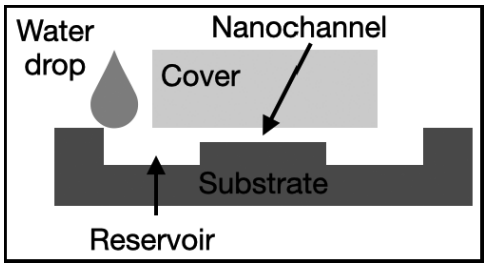

Figure 1: Sketch of cross-sectional view of the sample.

Figure 1 shows a cross-sectional view sketch of the nanochannel sample. The nanochannels, between two reservoirs, are ~ 2 cm long, 10 μm wide with 10 μm spacing between two adjacent channels. The channel height is 59 nm. The nanochannels were closed by bonding two wafers together. The fabrication process started from a silicon (Si) wafer — then ~ 3 μm thick photoresist (PR) was spin-coated and patterned through a standard photolithography process. The wafer was etched down for a certain depth to form open nanochannels, using patterned PR as mask. After removing the remaining PR, ~ 1 μm thick SiO_2 film was deposited using plasma enhanced chemical vapor deposition (PECVD), and was patterned by standard photolithography followed by dry etching, to serve as the hard mask for deep Si etching (Bosch process) for reservoirs (~ 30 μm deep). Then, after removing the remaining PECVD SiO_2 film using buffered oxide etchant, a new 300 nm thick PECVD SiO_2 film was deposited prior to bonding. The nanochannels were closed by bonding a glass piece above the channels using standard anodic bonding. The image from atomic force microscope (AFM) showing channel profile prior bonding was shown in Figure 2.

To perform wicking experiments, the sample was cleaned using deionized (DI) water, followed by oxygen plasma cleaning for 30 min. A DI water drop was placed in the reservoir, and water would wick into the channels, flow forward to fill the channel until reaching the other end. This wicking process was recorded using high speed camera

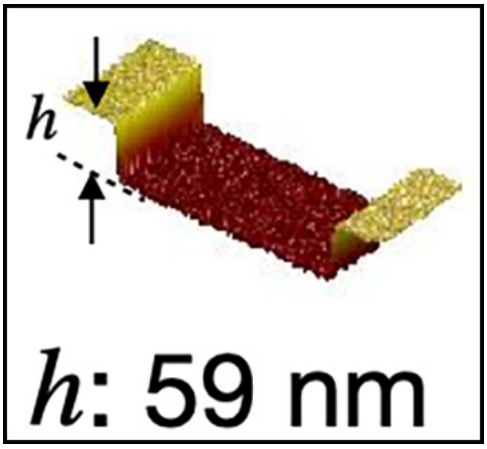

Figure 2: AFM image of channel profile prior bonding.

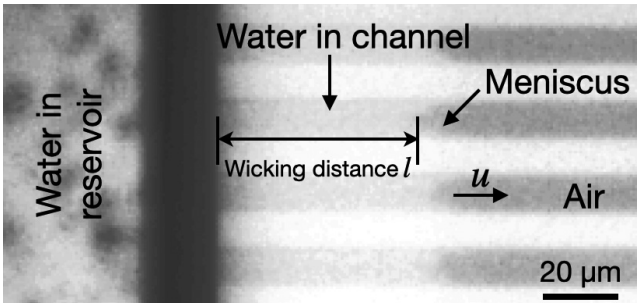

Figure 3: A typical image of the wicking from high speed video.

from the top. From the obtained video, the wicking distance l can be obtained by measuring the distance between the entrance and the position of the meniscus. Figure 3 shows a typical high speed image of the wicking. After finishing one test, the sample was heated to ~ 200°C on a hot plate in the open air to dry, which would take several minutes up to several hours. The wicking experiments for each sample were conducted at least four times to ensure repeatability.

The wicking distance (l) is proportional to square root of wicking time ($t^{1/2}$), as predicted by the simplified analytical solution (Eq. 1) of Navier-Stokes equation for wicking in a low specific ratio (height << width) rectangular cross-sectional channel [2].

$$l = \sqrt{\frac{h^2 \Delta P}{6\mu}} \cdot t^{1/2} = C \cdot t^{1/2}$$

where h is the channel height; ΔP is the total pressure difference driving the wicking; and μ is the fluid dynamic viscosity.

Figure 4 shows experimental results for both 59 nm and 1015 nm channels. As expected, the wicking distance is linear to square root of time with a slope C of 1.00 mm/s$^{1/2}$. As shown in Eq. 1, this slope is a function of channel geometry (height), liquid property (viscosity), and

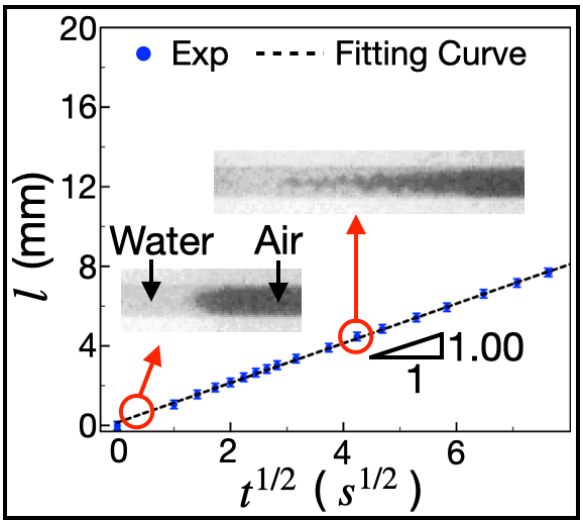

Figure 4: Variation of wicking distance with square root of time.

pressure difference. As both channel height and viscosity are known, the pressure difference can be calculated from experimentally obtained slope.

There are two potential contributions to the total pressure difference driving the wicking: disjoining pressure (due to the intermolecular interactions) and capillary pressure (due to the curvature of the meniscus). An interesting observation of wicking in 59 nm channels is that two types of meniscus were observed: regular-curved shape and wedge shape (Figure 4). The regular-curved meniscus occurred only within the first few hundreds of microns from the entrance. Beyond this initial distance, water was seen to flow much faster at the corners, forming the wedge-shape meniscus, which also led to air or vapor being momentarily trapped within the wicking liquid front. The different meniscus shape implies varied capillary pressure, however, constant slope C was observed during entire wicking process. Thus, capillary pressure was not major contribution to the total pressure difference; while disjoining pressure drove the wicking. With the estimation of capillary pressure in Ref. [1] and Eq. 1, disjoining pressure was calculated as 1.51 MPa. This is a first experimental characterization of disjoining pressure of water in SiO_2 nanochannels.

Conclusions and Future Steps:

We studied the water wicking in SiO_2 nanochannels, from which the disjoining pressure was characterized as 1.51 MPa in 59 nm channels.

References:

[1] A. Zou, S. Poudel, S.C. Maroo, arXiv preprint arXiv:2010.09928 (2020).

[2] B. E. Rapp, Microfluidics: Modelling, Mechanics and Mathematics. Micro and Nano Technologies, Oxford: Elsevier, 2017.